ELSEVIER

Contents lists available at ScienceDirect

Renewable and Sustainable Energy Reviews

journal homepage: www.elsevier.com/locate/rser





Magnitude and distribution of the untapped solar space-heating resource in U.S. climates

A.R. Rempel ^{a,*}, A.W. Rempel ^b, S.M. McComas ^c, S. Duffey ^d, C. Enright ^c, S. Mishra ^e

- ^a Environmental Studies Program, University of Oregon, Eugene, OR 97403, USA
- ^b Department of Earth Sciences, University of Oregon, Eugene, OR 97403, USA
- ^c Department of Landscape Architecture, University of Oregon, Eugene, OR 97403, USA
- ^d Department of Planning, Public Policy, and Management, University of Oregon, Eugene, OR 97403, USA
- e Department of Mechanical, Aerospace, and Nuclear Engineering, Rensselaer Polytechnic Institute, Troy, NY 12180, USA

ARTICLE INFO

Keywords: Space-heating decarbonization Solar energy Renewable resource evaluation Diffuse solar radiation Climate-responsive design Passive solar heating

ABSTRACT

Space heating is the single greatest source of building-related greenhouse gas emissions in the industrialized world, giving urgency to the development of strategies for carbon-free heating. Recent advances have shown that the direct capture, storage, and deployment of solar energy, without conversion to electricity, has considerable potential to address space-heating needs even in cold and cloudy climates. However, the solar energy available for direct heating at climatic and metropolitan scales is both unquantified and widely assumed to be negligible, impeding further investigation, development, and policy responses. To estimate the magnitude and distribution of solar resources concurrent with space-heating needs, we spatially integrate datasets characterizing solar radiation, outdoor temperature, and heating energy use across U.S. climates. Results show that the median resource incident upon collectors of residential scale (10 m²) and distribution is much greater than previously realized, equaling 7 MWh per household annually; by comparison, the median household heating need is currently 10.3 MWh. Unexpectedly, cloud-diffused solar radiation accounts for over one-quarter of this resource in all but semi-arid climates. Metropolitan residential resources exceed 5 TWh in areas including Detroit and Boston (cold continental), Washington D.C. (humid subtropical), Seattle and San Francisco (Mediterranean), and Denver (semi-arid), and national resources exceed 750 TWh annually, compared to approximately 1200 TWh of annual heating need. Current technology is able to capture and retain over half of a direct solar heating resource, revealing that the untapped U.S. solar heating potential is comparable to one-third of the national residential space-heating need and implying that analogous resources exist in analogous climates worldwide.

1. Introduction

Space heating of residential buildings consumes one-tenth of all site-delivered energy in the developed world, exceeding that of lighting, appliances, air conditioning, cooking, and water heating combined [1]. This immense quantity – over 4PWh annually among International Energy Agency member countries – represents nearly 1 Gt of greenhouse gas emissions each year [1,2]. Extensive effort has accordingly been devoted to improving building envelopes, increasing mechanical heating efficiency, and expanding renewable energy supplies [3–5]. At the same time, growth in built floor area [6,7], and growth of electricity demand beyond that of renewable supplies [8–10], are causing total space heating energy use and emissions to resist decline [11,12]. In response, the Intergovernmental Panel on Climate Change has called

urgently for strategies to reduce mechanical space heating needs [13] (Supplementary Information: Sec. S1; Figs. S1-1, S1-2).

Recent advances suggest that direct solar heating has considerable potential as such a strategy. In this approach, solar radiation is collected through windows and skylights, partly for immediate warming of air and partly for storage in materials for release during cooler hours (Fig. 1). Hourly and daily variations in solar resources and outdoor temperatures are tempered by sustained thermal delivery from these storage materials, causing solar heating systems to operate over time scales of several days or longer; they are not expected to provide heat on demand, nor always to provide thermal comfort [14,15]. Instead, they typically operate alongside mechanical heating systems: a direct solar system collects, stores, and delivers as much energy as possible (or as needed), diminishing the load on the mechanical system, while

E-mail address: arempel@uoregon.edu (A.R. Rempel).

Corresponding author.

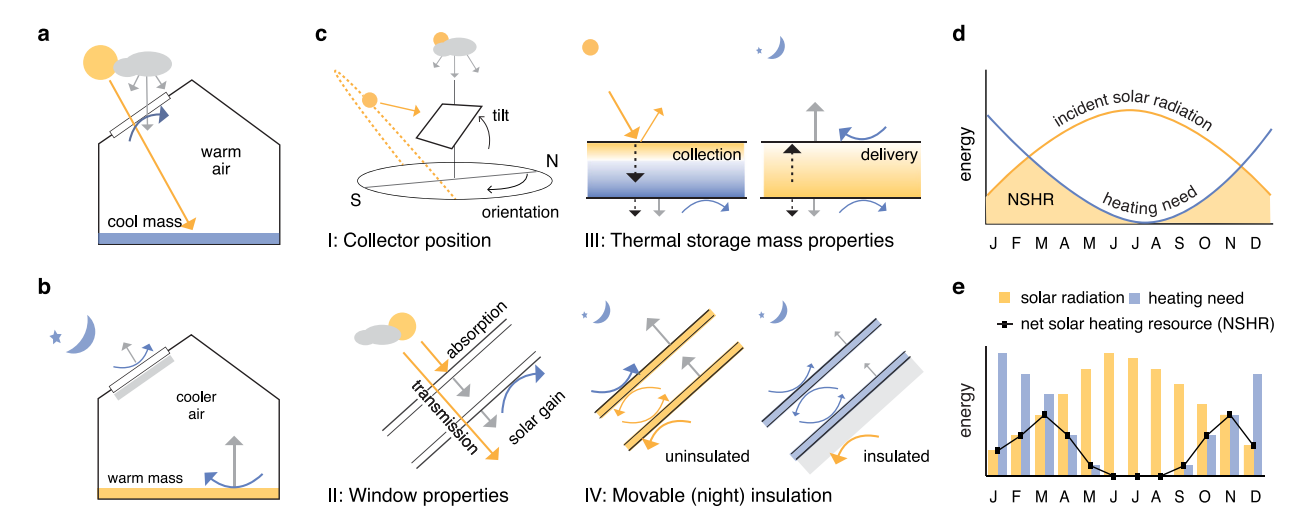


Fig. 1. Direct solar heating system operation. Arrows with solid straight lines indicate radiation; those with solid curved lines show convection; and those with dotted lines show conduction. Some processes are omitted for clarity. (a) Direct solar heat collection, in which direct (beam) solar and/or cloud-diffused radiation enter a building space through skylights or windows, partly warming air and partly warming cool materials, including dedicated thermal storage mass. (b) Nighttime heating of the space by warm materials through radiation and convection, with collector heat loss limited by movable (night) insulation. (c) Components: (I) Collector oriented and tilted to maximize exposure to climate-specific solar radiation during the corresponding heating season, shown for the Northern hemisphere; (II) Collector glass with a high solar heat gain coefficient (SHGC), a value that quantifies the proportion of incident solar radiation conveyed to the interior through transmission, surface radiation, and convection; (III) Thermal storage mass with properties that allow it to return heat in the desired pattern (i.e. briefly and intensely, over a long period of time at lower intensity, or between these extremes), showing the possibility of heat delivery or loss by the non-collecting face; (IV) Movable insulation for limitation of nighttime heat loss through collector glass. (d) Net solar heating resource, conceptually, shown as the monthly solar radiation incident on a collector surface limited by the heating need. (e) Net solar heating resource pattern typical of a cold continental climate

Nomenclature and abbreviations	
HDD	Heating degree-days
HDD _{18.3°C}	HDD calculated from a base temperature of $18.3^{\circ}\mathrm{C}$
\mathcal{H}_i	Heating season severity of month i (HDD _{18.3°C})
NSHR_{lpha}	Net Solar Heating Resource on a surface of area α (MWh, TWh)
NSRDB	National Solar Radiation Data Base
I_i	Incident solar radiation on a tilted surfaces (W/m^2)
$I_{ m direct}$	Direct solar radiation intensity (W/m ²)
$I_{ m diffuse}$	Diffuse solar radiation intensity (W/m²)
RECS	Residential Energy Consumption Survey
RSE	Relative Standard Error
SHGC	Solar heat-gain coefficient
TMY2	Typical Meteorological Year 2 (1960–1990)
TMY3	Typical Meteorological Year 3 (1975–2005)
TMYx	Typical Meteorological Year Next (2004–2018)
FTMY-2020	Future Typical Meteorological Year (2020)
α	Collector area (m ²)
ϕ	Collector orientation (degrees)
heta	Collector tilt (degrees)
Ψ	Space-heating energy use intensity (kWH/HDD $_{18.3^{\circ}\mathrm{C}}$)

the mechanical system remains available to provide supplemental heat when it is needed to reach the comfort zone.

Direct solar systems built according to U.S. guidelines that were established in the 1970's showed limited abilities in cool, cold, and cloudy climates [16,17], but several developments since that time have

improved performance dramatically. In the mid-1980's, field investigations throughout Europe showed that the solar energy captured for space heating by buildings in coastal northern climates greatly exceeded that captured in sunnier southern climates, a surprising finding ultimately explained by the fact that the longer, cloudier heating seasons extended into spring and fall months with numerous hours of daylight [18-20]. Cloud-diffused solar radiation accounted for much of the solar heating resource in these climates, contributing to the initial surprise. In the 1990's and 2000's, however, researchers realized that diffuse solar radiation emanates largely from the upper portions of the sky dome, rather than evenly from all directions or from the direction of the sun itself [21-23] (see also Supplementary Fig. S3-2). The sloping glass roofs characteristic of northern European conservatories had therefore been well-positioned to collect it. These studies established the potential of direct solar heating in cloudy, rainy, and northern climates, as well as the necessity of tilting collectors to intercept high-altitude diffuse radiation.

Independently, field work in cold continental Alaskan climates revealed the necessity of sizing thermal storage materials for the available solar resource [24], correcting earlier recommendations for the use of uniform "mass to glass" ratios [16] that promoted excessive thermal storage in climates with low winter solar intensity. Related work has shown, further, that thermal storage materials may be chosen, sized, and configured both to accommodate the solar resource available and to release heat in the pattern desired. In this way, heat delivery may alternatively be focused soon after solar collection begins, in a pattern desirable for daytime workplaces; soon after collection ends, for evening-occupied residences; or extended throughout the coolest hours of the night [25,26]. Additionally, the ongoing development of new glass materials and glazing assemblies (i.e., composites of glass, glass coating, and gas layers) continues to improve solar heating performance by providing collectors that increasingly allow high solar heat gain while limiting interior heat loss [compiled in 27], and the importance of movable insulation to limit heat loss further at night has now been well-established [summarized in 14].

Incorporation of the progress above into high-performance direct solar heating systems has been greatly facilitated by the concurrent development of building energy simulation tools, such as EnergyPlus [28,

29], that employ contemporary solar radiation models [21], angleand wavelength-specific optical and thermal representation of glazing assembly performance [27], and rigorous simulation of time-dependent material thermal behavior [30]. The performance of the resulting systems, often accompanied by field validation, has now been documented in numerous studies [e.g. 31-35]. Additionally, new tools for optimization [e.g. GenOpt 36] and control simulation (e.g. the Building Control Virtual TestBed [37] and the MATLAB-EnergyPlus Co-simulation Toolbox [38]) have facilitated detailed explorations of site- and buildingspecific system configurations, control strategies [39], and performance potential, reviewed most recently in [34]. As a result, direct solar systems are now expected to collect and retain 55% or more of the solar resource incident upon their collectors, even in cloudy climates, with further gains anticipated [18,39]. For context, solar collection performance and heat retention performance of current technology are documented for several contrasting climates in the Supplementary Information (Sec. S2.1, S2.2; Fig. S2-1, S2-2). Also included are the estimated costs of residential-scale direct solar heating systems comprised of commercially available materials, including framing with which the collector is positioned as desired, as is typical [e.g. 31,39]. These costs are now comparable to those of other residential-scale renewable energy additions [40], requiring initial investments of approximately \$10,000 per system and delivering energy at 11-18 U.S. cents per kilowatt-hour [41], detailed in Sec. S2.3 and in Table S2-1.

Still, direct solar heating systems remain rare in developed countries [2]: fewer than 0.2% of U.S. households reported solar heating use in 2018 [42], for example. Additionally, direct solar heating is neither recommended nor rewarded by prominent building energy efficiency codes, standards, rating systems, or programs, including the International Energy Conservation Code [43], the International Green Construction Code [44], ASHRAE Standard 90.1 [15], Leadership in Energy Efficiency Design (LEED) [45], the U.S. Department of Energy Building America Program [46], the U.S. Environmental Protection Agency Energy Star Program [47], and the Passive House Institute U.S. [48]. Together, these reflect the low confidence that currently exists in the quantity and consistency of solar resources when heat is needed [17,49,50]. Solar radiation useful for direct space heating is, as a consequence, a potentially valuable but virtually untapped resource. Because its magnitude, distribution, and consistency are entirely unknown, progress at metropolitan, regional, and national scales has little incentive to proceed. The objective of the work presented here is therefore to quantify solar resources that exist when heat is needed, and that are therefore available to be intercepted by appropriate collector surfaces, across diverse climates and metropolitan areas. In this way, this work is intended to support future research, development, and policy efforts.

The direct solar heating resource is distinct from photovoltaic resources [e.g. 51,52] in its occurrence exclusively during cool months, and primarily in cool climates, and it is distinct from solar thermal resources, particularly those of interest for concentrated solar power [e.g. 53], in the substantial contribution of cloud-diffused radiation. Because of these distinctions, the direct solar heating resource is well-positioned to add to, rather than compete with, other renewable resources. The ability of direct solar heating to use diffuse radiation effectively, familiar in the ability of a sloped automobile windshield to warm the interior on cool cloudy days, gives it the potential to supplement both photovoltaic electricity generation and heat pump operation during a climate's coolest months. Electric heating and cooking loads are typically highest during these months [54], while photovoltaic electricity generation is typically lowest, since daylight hours are typically fewest and proportions of direct solar radiation are often least [55,56]. Heat pump efficiency is also lowest during the coldest months of the year [57]. As a result, the partial offset of heating demand during these months by solar space heating has the potential both to diminish heat pump loads and to free photovoltaic production for other uses,

expanding the range of building energy end-uses met by renewable resources.

This work reveals the magnitude and distribution of the direct solar heating resource for the first time. To find these quantities, we integrated spatial and temporal databases documenting weather, solar radiation, space-heating energy use, and household density patterns to quantify solar radiation concurrent with space-heating needs, using U.S. datasets for their completeness and accessibility. The resulting 'net' solar heating resources (i.e., excluding solar radiation in excess of need; Fig. 1d,e) are unexpectedly extensive and consistent even in cold, humid, and cloudy climates, where annual values above 7 MWh incident upon residential-scale collectors are typical and the median interannual variation is less than 15%. For comparison, recent estimates find U.S. household average space-heating energy consumption to be 10.3 MWh per year [58]. Strikingly, the total U.S. national residential resource available to be intercepted exceeds 750 TWh per year, with median interannual variation of less than 5%, compared to total annual U.S. residential space heating needs of 1200 TWh [58]. As a result, at current solar heat collection efficiencies of greater than 50% (Supplementary Information Sec. S2), this virtually untapped resource corresponds to approximately one-third of the total U.S. residential heating energy need.

2. Materials and methods

The methods below describe the integration and evaluation of datasets that characterize space heating energy needs and concurrent solar resources spatially and temporally across the U.S., focusing on the years 2020 and 2000. Results are reported at monthly intervals to reflect both the operational timescales of direct solar heating systems (i. e., several days or longer) and the intervals over which weather and solar radiation are consistent from year to year.

2.1. Space-heating energy use datasets

Annual values of U.S. residential space-heating energy consumption were obtained from the U.S. Residential Energy Consumption Surveys (RECS) conducted in 2001 and 2015 [58,59]. Data from 2001 were used for year 2000 estimates, while 2015 data, the most recent available, were used for 2020 estimates (see Sec. S3.1 for a table of all datasets and their temporal alignment). These data represent actual, rather than simulated or archetypal, heating energy use and were chosen to describe current U.S. heating practices as accurately as possible; for example, adaptation of thermal comfort preferences to local climate conditions has been found to influence space-heating energy use noticeably [60]. RECS values used here, distinguished only by major climate zone, encompass all residential types, sizes, and ages; disaggregated data are protected from direct use by the Confidential Information Protection and Statistical Efficiency Act [61,62]. Additionally, RECS data were reported by different climate zones in 2001 and 2015: 2001 climate zones were defined exclusively by average annual (1971-2000) heating and cooling degree-days (HDD and CDD, respectively), where one heating degree-day represents a 24h average outdoor air temperature of one degree below a given baseline temperature, often 18.3 °C [63,64]. In contrast, 2015 climate zones [65] incorporated precipitation and seasonal temperature patterns as well as annual HDD and CDD (compare Fig. S3-3a and b). Since these climate zones largely followed county boundaries, except in western states where some followed drainage basins, U.S. county maps [66] were used to construct shapefiles representing the boundaries of both major climate zone sets in ArcGIS 10.5 [67] to facilitate subsequent intersections of these data with the others. These and all subsequent maps used the USA Contiguous Albers Equal Area Conic projection.

2.1.1. Uncertainty in space-heating energy use datasets

All RECS data were reported as means with relative standard errors [58,59,63,65], and approximately 5000 households were surveyed in each year [63,65], allowing 95% confidence limits for the means to be estimated as $\pm 1.96 \times RSE$ [68].

2.2. Weather datasets

Typical meteorological year 3 (TMY3) files, the majority of which characterize 1991-2005 data [69], were used to represent weather conditions across the U.S. for the year 2000. For 2020 analyses, TMY2 (1961-1990) files [70] were processed into future TMY (FTMY) 2020 files using CCWorldWeatherGen v1.8 [71], one of the principal tools available for generating future weather files for building energy simulation [72]. This procedure transforms 1961-1990 baseline data into future year estimates using version 3 of the Hadley Centre Coupled Model (HadCM3) under parameters of the medium-high, or "business as usual", A2 emissions scenario [71,73]. Annual HDD_{18.3 °C} of the resulting FTMY-2020 files corresponded closely (r(237) = .996, p < .00001) to those of the same stations recently reported in "TMYx" weather files derived from 2004–2018 measurements [74] (Fig. S3-1b), confirming the validity of the FTMY-2020 files and allowing source data for the TMYx 2004-2018 files to be used in uncertainty estimates (below). Geographic boundaries of the sectors represented by each of the individual (609) TMY3 and (239) FTMY weather files were established on the basis of proximities and elevation similarities of 10 km × 10 km gridcells to individual weather stations, weighted to favor stations with lower measurement uncertainty, according to National Renewable Energy Laboratory methods [75]. Station latitudes and longitudes were taken from station weather files, and elevations were determined from U.S. Geological Survey topographic data [76].

2.2.1. Uncertainty in weather datasets

Among TMY3 weather files, annual $HDD_{18.3\,^{\circ}C}$ have previously been reported to fall within 5% (95% confidence level) of average annual HDD_{18.3 °C} in the corresponding long-term data [69]. Independently, the National Climatic Data Center estimated the 30-year variability in the temperature data of each TMY3 source weather station [77]; among the TMY3 stations used here [75], the mean standard deviation in monthly temperature (± SEM) was 1.73±0.75 °C. FTMY-2020 weather files, in turn, incorporated uncertainty related to (i) the validity of the underlying HadCM3 global circulation model forcing and output, (ii) the HadCM3 atmospheric grid resolution of 2.5° latitude × 3.75° longitude (corresponding to distances between grid points of approximately 300 km in the continental U.S., comparable to the 242 km mean spacing between each TMY2 station and its five nearest neighbors), and (iii) the validity of the morphing procedure, principally limited by its inability to represent the increasing frequency of extreme weather events and intensifying microclimate effects such as urban heat islands [73]. Because of the resulting inability to quantify FTMY-2020 error directly, as well as the close correspondence between FTMY-2020 and TMYx 2004-2018 files, individual 2004-2018 years of TMYx source data were acquired from the National Oceanographic and Atmospheric Administration (NOAA) Integrated Surface Database (ISD) [78] and used to estimate effects of interannual temperature variability on space-heating energy needs, collector tilt optima, and net solar heating resources (detailed in Sec. S3.6, Fig. S4-6, and Sec. S5).

2.3. Space-heating energy intensity (ψ) and heating need

Relationships between annual space-heating energy use (kWh) and annual heating season severity in normal heating degree-days (HDD_{18.3 °C}), here described as space-heating energy use intensities ψ (kWh/HDD_{18.3 °C}) per household, were next found for each major RECS climate zone. This allowed subsequent estimation of heating energy use both at monthly intervals and at the resolution of TMY3-

and FTMY-2020 weather file sectors (Fig. S4-1). Because RECS survey data were self-weighted by housing density [63,65], census-reported household distribution data were used, in addition, to eliminate this influence. To reveal the combination of household density, annual space-heating energy use, and annual HDD $_{18.3}$ °C within each weather file sector, household distributions at the block-group scale from 2000 and 2010 (the most recent available) U.S. census maps [79] were spatially intersected with TMY3 and FTMY-2020 sector boundaries (Fig. S4-1), representing weather data from 2000 and 2020 [73,80], respectively, and with corresponding RECS 2001 and 2015 climate zone boundaries (Fig. S3-3) representing space-heating energy use [81,82].

Space-heating energy use intensities ψ (kWh/HDD $_{18.3}$ $_{^{\circ}\text{C}})$ were then found from:

Annual space heating energy use (kWh) =
$$\psi \sum_{j} \sum_{i=1}^{12} \binom{\text{Residences}}{\text{in sector}_{j}} \times \mathcal{H}_{i}$$
, (1)

where \mathcal{H}_i represents the HDD_{18.3 °C} for month i, and the outer sum is taken over each of the TMY3 or FTMY-2020 geographical sectors for the years 2000 and 2020, respectively. Ninety-five percent confidence intervals of the resulting space-heating energy use intensities were estimated from RECS-reported relative standard errors for annual heating energy use and heating degree-days, per surveyed house-hold [58,59], using Fieller's method [83] (tabulated in Fig. S3-3). To estimate monthly space-heating energy needs within each TMY3 and FTMY-2020 sector, the space-heating energy intensities ψ found above (kWh/HDD_{18.3 °C} per household) were multiplied by \mathcal{H}_i in each corresponding sector.

2.4. Solar radiation datasets

Individual years of hourly direct normal and diffuse horizontal radiation data, as well as solar zenith and azimuth angles, were acquired from the 1991–2005 National Solar Radiation Database (NSRDB) update [84,85] for use in finding optimal tilt angles for solar-collecting glass at the scale of TMY3 and FTMY-2020 weather file sectors. Solar data modeled at 0.1° resolution from Geostationary Operational Environmental Satellite (GOES) imagery by SolarAnywhere, available publicly for 1998–2009 [86], were then used to estimate solar radiation incident on surfaces of optimal tilt among the lower 48 states and Hawaii. Alaskan estimates, however, instead used NSRDB solar data for the same time period (1998–2009) [87], modeled from surface observations of cloud cover [88], due to the inability of GOES imagery to resolve cloud cover in sufficient detail at high latitudes.

2.4.1. Uncertainty in solar radiation datasets

In validation tests of the models (METSTAT and SUNY-A) used to create the NSRDB and SolarAnywhere datasets, respectively, mean bias errors for monthly mean daily totals of global horizontal radiation ranged from -0.06% to 1.73% of measured values, while root mean square errors ranged from 5% to 8%, comparable to instrument-related uncertainties in the measurements themselves [84,89]. Since short-term errors tended to cancel out over each year, however, uncertainties in annual totals were found to be less than 2% [84], causing interannual variability rather than model error to be the primary source of uncertainty in solar data [90]. Because monthly solar radiation totals were non-normally distributed in both datasets (evaluated with one-sample Kolmogorov–Smirnov tests using the MATLAB function kstest [91]), all results dependent on solar radiation data are expressed as medians, and uncertainties are expressed as median absolute deviations or as approximate 95% confidence intervals [92].

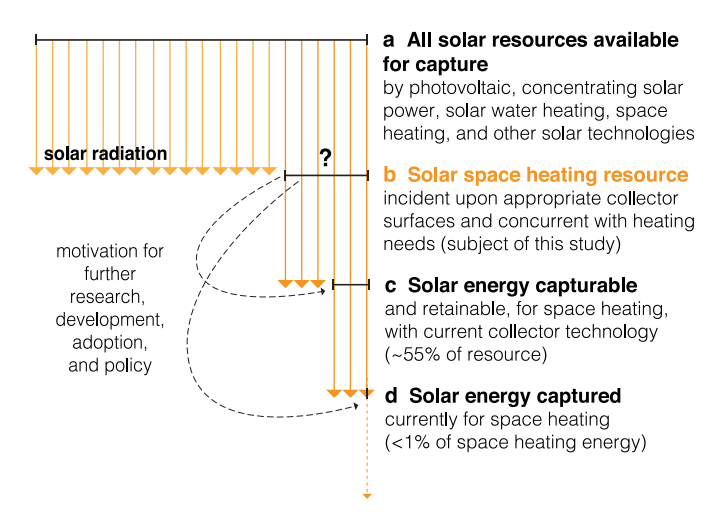


Fig. 2. Study scope. (a) Solar energy resources (down arrows) suitable for capture by numerous technologies unrelated to space heating have been most recently reviewed by Kannan and Vakeesan [93] and by Kabir et al. [94]. (b) Solar resources suitable for space heating have not previously been investigated and are the subject of this study, with the goal of providing a theoretical framework for further research, development, and policy. (c) With current technology (i.e. high solar heat gain glass, night insulation, thermal storage), approximately half of the solar energy incident upon a space-heating collector may be captured and retained in diverse climates [e.g. 18,31,39, corresponding evidence is reviewed in detail in the Supplementary Information]. (d) Despite the ability to capture half of the incident solar resource, fewer than 1% of U.S. households employ solar space heating even at supplementary levels [42], due in part to lack of confidence in solar resources in cool, cold, and cloudy climates [49].

2.5. Calculations of solar radiation on tilted surfaces

To calculate total (diffuse + direct) solar radiation I_i incident upon tilted surfaces, the model of Perez et al. [21] was chosen based on its prior validation in diverse U.S. cities [95] and in our own previous field studies [31,39,96]. Simple geometrical arguments were applied to resolve direct solar irradiation onto surfaces of given tilt, solar azimuth, and zenith angle, yielding hourly values for $I_{\rm direct}$. The diffuse component $I_{\rm diffuse}$ was evaluated using reported hourly diffuse irradiation levels while accounting for the effects of local elevation, zenith angle, and variations in sky clearness following the EnergyPlus AnisoSkyMult routine [30]. Calculation details are provided in Sec. S3.3.

2.6. Calculations of optimal tilt

To find optimal solar collection tilts for each TMY3 and FTMY-2020 sector, the MATLAB golden section search routine fminbnd [91] was used to determine the tilts of $10\,\mathrm{m}^2$ surfaces that received maximum incident solar radiation, limited monthly by space-heating energy needs, during each sector's heating season (i.e. months with $>55\,\mathrm{HDD}_{18.3\,^\circ\mathrm{C}}$). South-facing orientations were assumed for simplicity in describing metropolitan- and national-scale resources; on specific sites, however, non-south orientations may be equally or more favorable under certain conditions [14,31]. Median tilts among the optima found for each of the 15 years of the 1991–2005 NSRDB solar dataset [85] were then used in subsequent calculations of total and net solar heating resources.

2.7. Methodological limitations

2.7.1. Effects of dataset uncertainty

The principal sources of error in estimating net solar heating resources were (i) uncertainty in RECS-reported heating energy use [58, 59,63,65]; (ii) uncertainty in heating degree-days represented by FTMY-2020 [73] and TMY3 [77] weather files; and (iii) uncertainty in NSRDB-reported national solar radiation data [84,86,89]. The corresponding effects on calculated parameters were evaluated for 20

representative cities using 2020 data, followed by examination of the most influential factor at high resolution across the U.S. First, the influences of uncertainty in solar radiation and in space-heating energy needs on collector tilt optima were found; next, sensitivity to this variability was investigated directly by calculating NSHR values over collector tilts from 0° to 90° at 5° intervals. NSHR sensitivity to interannual variation in normal heating degree-days \mathcal{H}_i was then evaluated using uncertainty derived from individual years of 2004–2018 NOAA ISD weather data [78]. Finally, NSHR sensitivity to interannual variability in solar radiation was shown by estimating median absolute deviations in NSHR₁₀ for both 2020 and 2000 using individual years of SolarAnywhere data across the U.S. [86]. Calculation details are provided in Sec. S3.6.

2.7.2. Study scope

The scope and objectives of this study are to quantify (i) the spatial and temporal patterns of the incident solar resource useful for space heating; (ii) the collector tilts needed to intercept this resource effectively; and (iii) the interannual variation that may be expected (Fig. 2). This work then interprets the direct solar heating resources found in light of current collector performance, for context and relatability, but it does not attempt to quantify the performance potential of specific individual buildings or systems or to investigate factors that affect their performance; these are well-documented elsewhere (see [96-98] and references in the Introduction). Likewise, this study does not attempt to estimate the proportion of the resource that could be captured by the specific existing buildings of individual cities, affected by site-specific and changeable building forms and tree cover, though aggregate resources are estimated in the context of urban densities. Such higher-resolution analyses should soon be possible through physical or "bottom-up" urban building energy modeling [99], and ideally, this work will motivate such studies. At the present time, however, the available tools (e.g. CitySim [100], UMI [101], CityBES [102,103], City Energy Analyst (CEA) [104]) do not yet support the automatic, comprehensive creation of new surfaces (i.e. that are non-coplanar with existing building surfaces) in city models such as those that would reasonably be constructed for direct solar heating collectors. In addition, direct solar heating applications are not yet included with other energy conservation measures provided by programs designed for rapid city-wide analysis [e.g. 102]. As a result, such work is beyond the present scope.

3. Results and discussion

3.1. A new metric for solar heating resources

Direct solar heating resources have previously been expressed in terms of the Solar Savings Fraction (SSF), defined as the ratio of the space-heating energy saved by a solar-heated building to that consumed by an analogous conventional building in the same location [16,50]. Since this fraction tends to be highest in warm or sunny climates, however, and lowest in cold or cloudy climates, it misleadingly implies that direct solar heating provides less total energy in the latter [18, 19]. To correct this bias, we began by establishing a new metric to quantify solar radiation useful for heating in absolute terms: the Net Solar Heating Resource (NSHR $_{\alpha}$). A location's NSHR $_{\alpha}$ is a measure of the absolute solar radiation incident upon a surface of optimal tilt θ (degrees), orientation ϕ (degrees) and defined area α (m²) that is no greater than the simultaneous heating need (Fig. 1d, e). Here, monthly intervals were chosen for NSHR documentation to represent time spans at which weather and solar radiation data have sufficient interannual consistency that the resulting resource estimates will be meaningful for

To find monthly residential NSHR values, we first estimated monthly heating energy needs for typical households from two metrics: typical monthly heating-season severities \mathcal{H}_i expressed in normal

heating degree-days (HDD), where one HDD $_{18.3\,^{\circ}\text{C}}$ represents a 24h average outdoor air temperature one degree below the standard base temperature of $18.3\,^{\circ}\text{C}$ (65°F), and corresponding space-heating energy use intensities ψ , representing the energy used for each normal HDD (kWh/HDD $_{18.3\,^{\circ}\text{C}}$). Space heating energy use intensities, in turn, were calculated from concurrent values of space heating energy use, house-hold distribution, and outdoor air temperature data (see Section 2). Annual NSHR values were then found by summing monthly solar radiation values incident upon optimally tilted surfaces $I_i(\theta,\alpha)$, limited by the corresponding monthly heating energy needs:

$$NSHR_{\alpha, annual} = \sum_{i=1}^{12} \min \left[\psi \mathcal{H}_i, I_i(\theta, \alpha) \right], \tag{2}$$

where \mathcal{H}_i represents the sum of HDD_{18.3°C} for month i. For simplicity, orientation ϕ was held constant at 180° (i.e. due south in the Northern hemisphere), noting that direct solar heating performance is substantially less sensitive to orientation when the collector is tilted [14,31] instead of vertical [16]. Except where stated, NSHR values are reported for collector areas α of 10 m², a size frequently found among residential direct solar heating systems [31,39], and expressed as NSHR₁₀. For context, roof planes of this area with minimal shading, as well as favorable tilt and orientation for solar collection, have been found on approximately 80% of small (primarily residential) buildings surveyed in 128 U.S. cities [105].

3.2. Spatial patterns of heating energy need

Across much of the U.S., heating seasons (by convention, months with >55 HDD $_{18.3\,^{\circ}\text{C}}$) currently begin near the fall equinox (September 21–23) and extend past the spring equinox (March 21–22). Longer seasons, extending into May and including numerous weeks with more than 12 daily hours of sunlight, are found in the humid continental Northeast, Great Lakes, and Upper Midwest; semi-arid Mountain West; Mediterranean Pacific Northwest, and subarctic Alaskan climates (Fig. 3a; Fig. S4-1). Residences across much of the U.S. therefore have the potential to offset part of their mechanical heating energy with direct solar space heating for 5–9 months per year. Comparable time spans appear likely to persist over the next several decades, as annual HDD $_{18.3\,^{\circ}\text{C}}$ have declined from 2000 to 2020 by a median (\pm median absolute deviation) value of only $7\pm3\%$ among the weather stations shown [75] (compare Figs. S4-1a and b).

The 2020 and 2000 spatial intersections of outdoor air temperature data [73,80], corresponding residential space-heating energy use data [81,82], and household density [79] data revealed space-heating energy use intensities ψ (kWh/HDD_{18.3 °C}) per household that ranged from 2.7–5.7 kWh/HDD_{18.3 °C} in 2020 and 4.6–7.4 kWh/HDD_{18.3 °C} in 2000 (Fig. S3-3). While these values cannot be compared directly, due to differences in the major climate zones by which RECS data were reported (see Section 2.1), both sets reveal greater space heating energy use intensity (i.e., energy use per heating degree-day) in hot humid climates and correspondingly lower values in colder climates. These patterns are consistent with climatic variation in building practices as well as the adaptation of human thermal preferences to outdoor conditions (Sec. S3.4).

The combination of regional space-heating energy use intensities ψ (kWh/HDD_{18.3°C}) and local monthly heating degree-days \mathcal{H}_i (HDD_{18.3°C}) showed that monthly heating energy needs currently exceed 1.5 MWh per household from November through March across much of the U.S., with residences of the Northeast, Great Lakes region, Upper Midwest, and Alaska typically requiring \geq 2.25 MWh per month from December through February (Fig. 3). Heating needs are also appreciable in April, May, and October in the humid continental climates of the Northeast, Great Lakes, and Great Plains; in the Mediterranean Pacific Northwest; and in the semi-arid and subarctic Mountain West, showing that heating seasons in large areas of the U.S. extend into

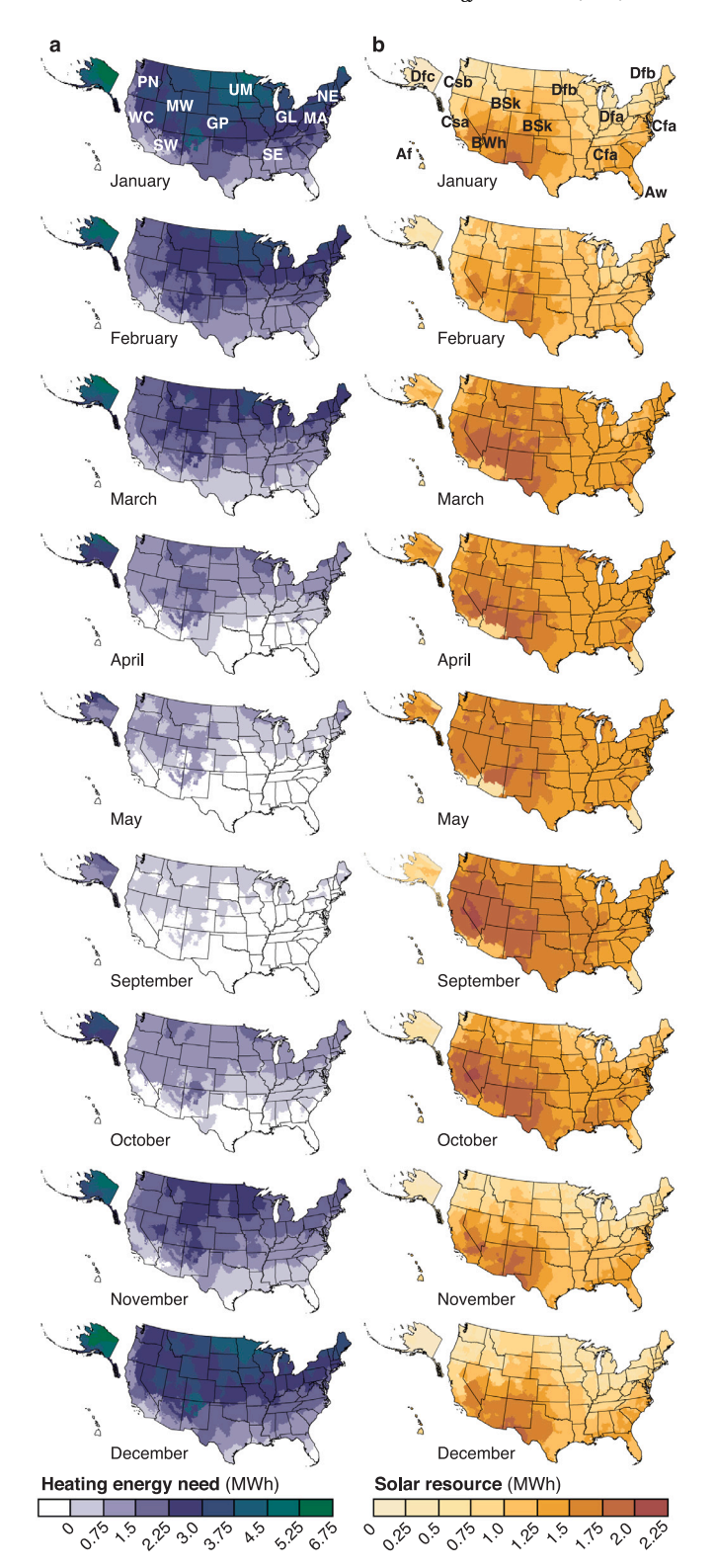


Fig. 3. Concurrence of solar resources and heating needs across U.S. climates, 2020. (a) Monthly heating energy needs (household means; MWh), calculated from 2015 residential space-heating energy intensities [81] (Fig. S3-3) and FTMY-2020 HDD_{18,3+C} [73] (Fig. S4-1). (b) Monthly solar resources (medians; MWh) [87], without limitation by need, on 10 m² surfaces of optimal tilt. Values for 2000 are shown in Fig. S4-2. Regions and climates: Tropical (Af and Aw; Hawaii and southern Florida, respectively); Semi-arid steppe (BSk; GP=Great Plains and MW=Mountain West); Hot desert (BWh; SW=Southwest); Humid subtropical (Cfa; MA=Mid-Atlantic and SE=Southeast); Hot-summer Mediterranean (Csa; WC=West Coast); Warm-summer Mediterranean (Csb; PN=Pacific Northwest); Hot-summer humid continental (Dfa; GL=Great Lakes); Warm-summer humid continental (Dfb; NE=Northeast and UM=Upper Midwest); Subarctic (Dfc; Alaska and high elevation MW).

months with 12 or more hours of daylight. Annually, household space-heating energy needs in cold climates (the Northeast, Upper Midwest, Great Lakes, and Mountain West) range from 12–24 MWh; those in the Great Plains and Mid-Atlantic regions range from 5–12 MWh; in the Pacific Northwest, 4–9 MWh; and in warmer arid and humid subtropical climates, 1–8 MWh. Typical annual household space-heating needs are tabulated for 239 U.S. cities in Dataset S2.

Comparison of 2020 and 2000 data shows, additionally, that U.S. total heating needs have declined by <0.5% per year over this time (compare Fig. 3 and Fig. S4-2), consistent with U.S. government projections of sustained high residential heating energy needs over the next three decades [11].

3.3. Optimal tilts for solar heat collectors

Previous work has shown that solar heat-collecting glass must be tilted in cloudy coastal climates to intercept maximum radiation during the heating season [31,39], revising earlier beliefs that vertical glass area, or the vertically-projected area of tilted glass, was of primary importance [16,50,106]. These findings were consistent with observations that solar radiation is increasingly emitted from the sky zenith as cloud cover increases [107] (Sec. S3.2; Fig. S3-2) and suggested for this study that optimal tilts for solar heat collection were likely to deviate substantially from vertical in climates with appreciable winter cloud cover. To investigate, we calculated solar radiation incident upon south-facing tilted surfaces as described above (Section 2), limited by each month's heating need, and used numerical optimizations to find the corresponding optimal tilts for its interception.

Under both 2020 and 2000 conditions, optimal tilts were found to be steep ($\geq 60^{\circ}$ above horizontal) only in sunny climates with little heating need, including the southernmost desert Southwest, tropical Hawaii, and parts of Texas and Florida. In these climates, optimal tilts responded to the low solar altitudes and limited cloud cover of the coolest months (December-February) (Fig. 4; Fig. S4-3). Across the humid subtropical Mid-Atlantic and Southeast, the humid continental Midwest, and parts of the semi-arid Mountain West, shallower tilts (50–60°) were optimal, with the shallowest optima (<50°) occurring in the cloudiest climates [55] and in those with the longest heating seasons: the Northeast, Great Lakes region, Pacific Northwest, and coastal Alaska. In these cool, cloudy climates, tilt optima reflected the high altitudes of both diffuse solar radiation in winter and direct radiation in late spring, when heat is typically still needed. At the same time, sensitivity analyses showed that these optima represented broad peaks, with tilts of $\pm 20^{\circ}$ from optimal values intercepting $\geq 95\%$ of the net solar heating resources found below (Fig. S5-2).

Correspondingly, across much of the U.S., diffuse radiation contributed more than one-quarter of the total net solar heating resource, with the highest proportions occurring in the spring months of February–May. Moreover, it provided over half of the total in the cloudy winters of the Great Lakes, Pacific Northwest, and Southern Alaska (Fig. 4; Fig. S4-3); only in the semi-arid Southwest did it provide less than one-fifth of the resource. The widespread importance of cloud-diffused energy to direct solar heating has not previously been understood: although diffuse radiation is readily transmitted through window glass [108], its high (i.e., bluish) color temperature is not perceived as warm [109,110], potentially explaining this omission [e.g. 16,50,106]. These results show, however, that diffuse radiation must be included in solar heating resource estimates across subarctic, continental, subtropical, and Mediterranean climate types.

3.4. Net solar heating resources

To reveal seasonal net solar heating resource patterns across all U.S. climates, including both direct (i.e., beam solar) and diffuse radiation, we used high-resolution (0.1°) solar data [86] to calculate radiation incident upon corresponding optimally tilted south-facing surfaces,

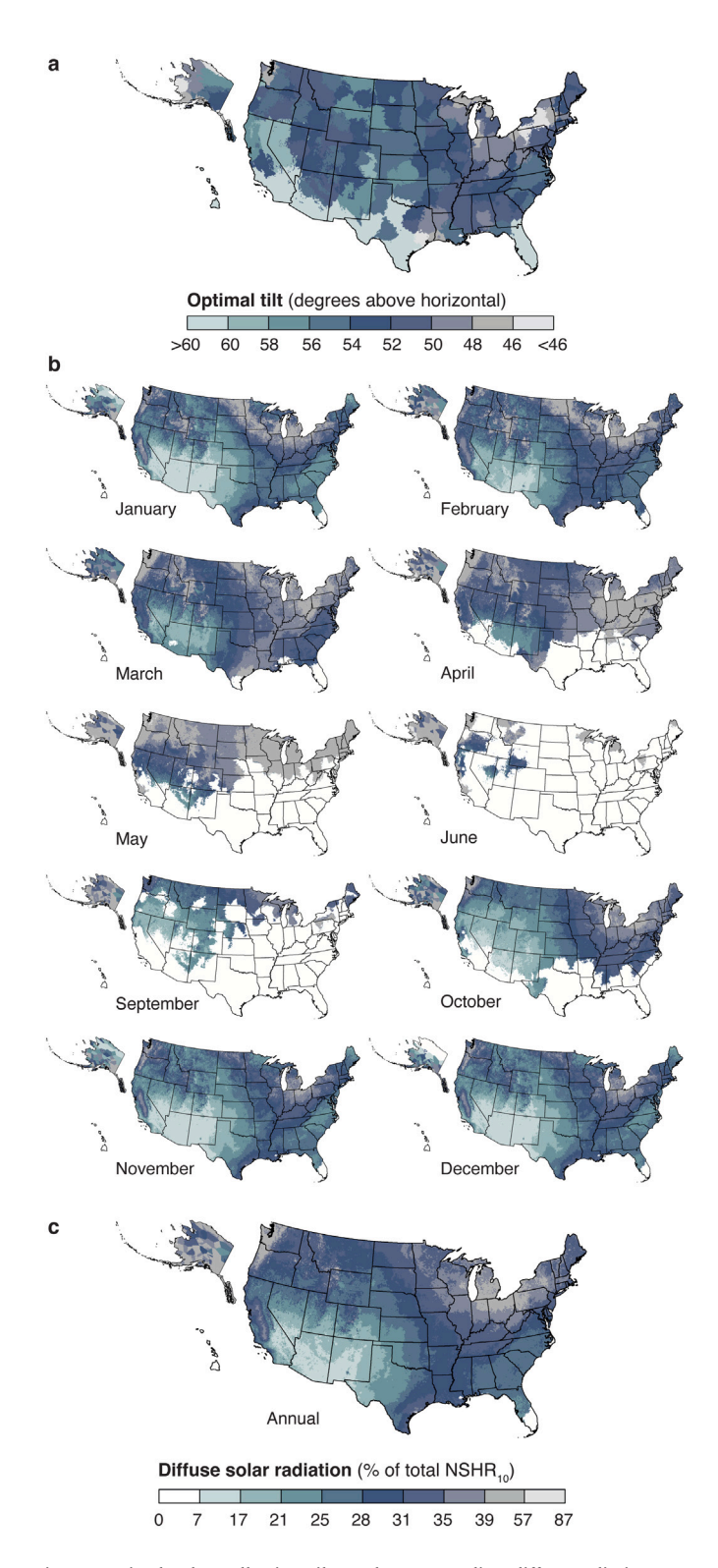


Fig. 4. Optimal solar collection tilts and corresponding diffuse radiation contributions, 2020. (a) Degrees of south-facing tilt (horizontal=0°; vertical=90°) for optimal direct solar heating collection found from maximizing interception of solar radiation [84] coincident with space-heating energy needs (Fig. 3). Shallower tilts correspond to cloudier heating seasons, in which diffuse solar radiation emanates to a greater extent from the sky zenith (Fig. S3-2), and/or to longer heating seasons in which high-altitude spring and fall solar radiation is useful. (b) Monthly percentages of the NSHR₁₀ provided by cloud-diffused solar radiation [86] on 10 m² surfaces of optimal tilt, showing correlations among tilt, seasonal cloud cover, and heating season length. (c) Annual percentage of the NSHR₁₀ provided by diffuse radiation. Analogous results for 2000 are shown in Fig. S4-3.

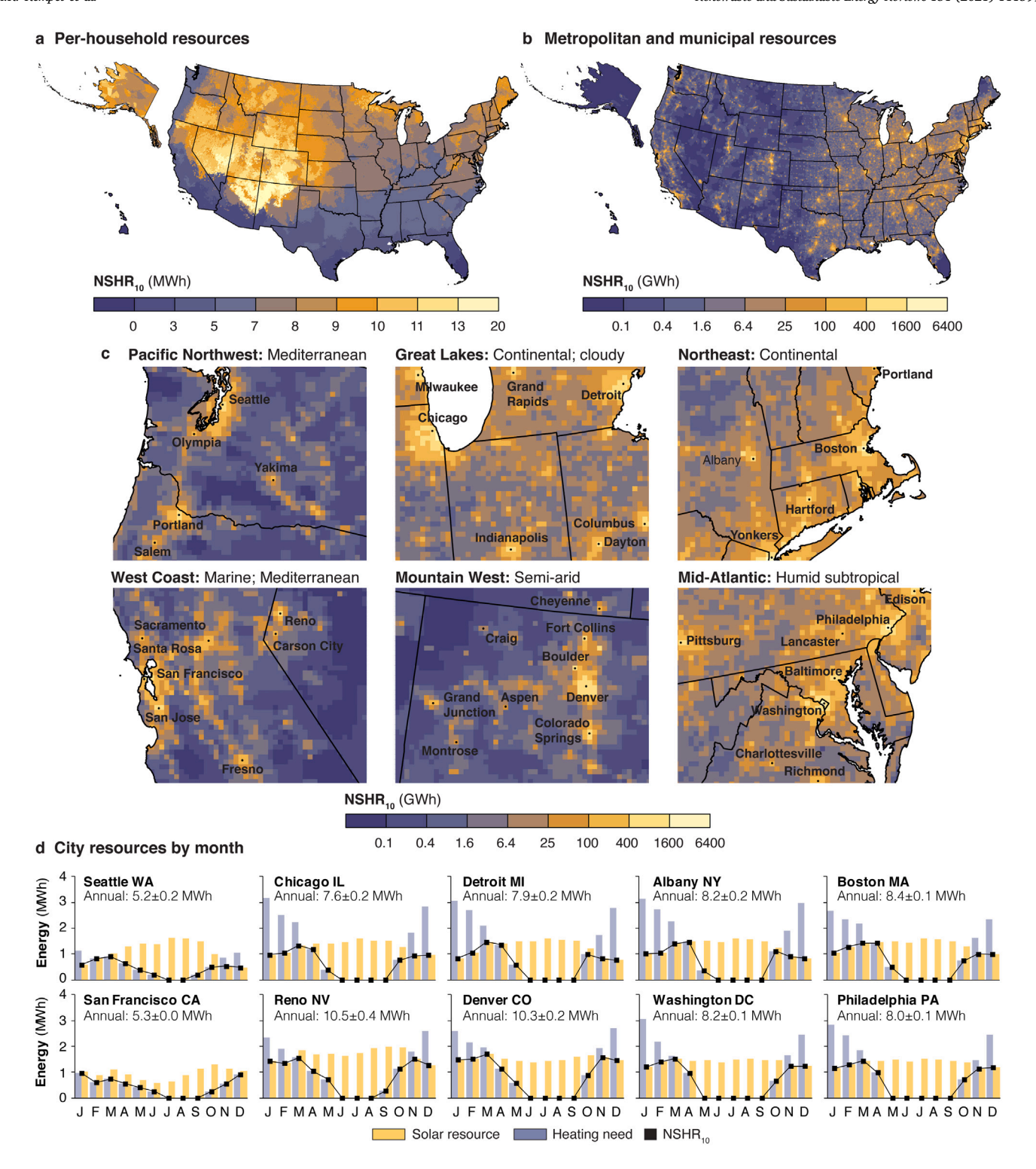


Fig. 5. Net solar heating resource: magnitude and distribution, 2020. (a) Annual solar radiation (MWh) useful for space-heating incident upon $10\,\mathrm{m}^2$ surfaces of optimal tilt expressed as medians per household by location. (b) Sum of median NSHR_{10} values (GWh) over all households in $10\,\mathrm{km} \times 10\,\mathrm{km}$ sectors. (c) Expanded views of b showing NSHR_{10} values (GWh) in portions of the Pacific Northwest (Mediterranean), Great Lakes (humid continental; cloudy), Northeast (humid continental), West Coast (marine), Mountain West (cold semi-arid), and Mid-Atlantic (humid subtropical) regions. (d) Characteristic patterns (MWh) among monthly heating needs (blue), solar resources (orange), and NSHR_{10} values (black) in cities representative of the regions and climates shown in (c), labeled with annual NSHR_{10} values and median absolute deviations. Analogous results for 2000 are shown in Fig. S4-4.

again limited by corresponding monthly heating needs, assuming $10\,\mathrm{m}^2$ collector areas. Under current (2020) conditions (Fig. 5; Dataset S2), peak values ($\geq 13\,$ MWh per household) occurred in the Mountain West and northern Southwest, as expected, while unexpectedly high values (8–11 MWh per household) were found in climates with long

heating seasons, including the humid continental Northeast and Upper Midwest, much of the northern Mountain West, and subarctic Alaska. Intermediate values of 7–8 MWh occurred throughout humid subtropical Mid-Atlantic and cloudier continental Great Lakes and Midwest areas, as well, representing the 2020 median U.S. household $\rm NSHR_{10}$

value of $7.0\pm0.4\,\mathrm{MWh}$ (see error discussion in Section 3.5 below). Also unexpectedly, resources of 5–7 MWh per household were found in much of the humid subtropical Southeast and Mediterranean Pacific Northwest and West Coast; for context, these values correspond to 80% or more of the heating need in coastal areas that have previously been regarded as too cloudy for direct solar heating [17]. In the warmest areas of the Southeast and Southwest, values of 3–5 MWh per household were found, comparable to the total heating needs of these areas; lower values occurred only in the tropical climates of south Florida and Hawaii. Together, these results reveal substantial solar heating resources across diverse cool, cold, and cloudy climates, including areas thought to have little solar heating potential [16,17,50], as well as resources in warmer climates sufficient to meet the majority of their heating needs. To provide further detail, 2020 NSHR $_{10}$ values are tabulated for 239 major U.S. cities in Dataset S2.

These household net solar heating resources are comparable to U.S. rooftop photovoltaic production potentials, recently estimated to range from approximately 7-11 MWh per year for small buildings [52]. While collection and retention efficiencies limit solar space-heating potential to about 55% of the resource value (Sec. S2), photovoltaic generation estimates assumed average rooftop areas six times larger than the 10 m² used here for heating calculations. National average household-level solar heating and solar photovoltaic potentials are therefore similar in magnitude. Of greater interest is the noticeable difference in the distribution of the two resources across U.S. climates. While both photovoltaic and solar heating resources show peak values in the semi-arid Mountain West, photovoltaic resources remain high across the southern U.S., declining in more northern latitudes and cloudier climates. Direct solar heating resources, in contrast, increase markedly with latitude, especially in the eastern and central U.S., and they surpass the national median value of 7 MWh throughout New England, the mid-Atlantic area, the Great Lakes region, and the Upper Midwest, as well as the interior Pacific Northwest (Fig. 5a).

To understand the concentration of net solar heating resources in metropolitan areas, we next summed these values over households within each 10 km × 10 km sector, an area chosen to maintain consistency with the 0.1° solar data grid. Although household access to solar resources within cities is expected to be unequal, these sums include all households equally for the following reasons. First, the current objective is to provide a transparent, useful estimate of solar resources available to be sought, independent of assumptions regarding the proportions of their ultimate capture (Fig. 2); only then can the magnitude of the resource inform policies regarding urban and building design that preserve solar access [see also 111,112]. Second, the vast majority of U.S. households currently occupy low-rise buildings: over 80% reside within single- or double-unit buildings in all but three metropolitan areas (New York City, Los Angeles, and San Francisco), and in those cities, that number nevertheless remains above 70% [113], showing that solar access among U.S. residences is, in fact, already widespread. Accordingly, a recent study of existing rooftops in U.S. cities found that the availability of minimally shaded 10 m² roof planes, suitably oriented for solar collection, is not significantly affected by urban density given the relatively low density of most American cities [105]. Finally, solar space-heating remains possible in the east-, south-, and west-facing units of higher-rise buildings through the use of vertical glass, which is able to collect a portion of the incident solar resource despite its non-optimal tilt [14], and through balcony sunspaces [114]. To preserve the goal of estimating resources, therefore, the values below consider all households to the same extent, allowing future investigations to interpret them in light of site-, building-, or city-specific constraints of interest.

Strikingly, metropolitan-scale estimates of the 2020 $NSHR_{10}$ exceed 5 TWh per year in numerous cities, including many in warm climates as well as those in populous areas of the Northeast, Mid-Atlantic, West, and Pacific Northwest (Fig. 5b, c, Dataset S2). Particularly in the Northeast, Upper Midwest, and Mid-Atlantic regions, the combination

of appreciable per-household resources and household density extending beyond city centers creates substantial aggregate metropolitan resources. Graphs comparing monthly heating needs with corresponding solar resources for median households in ten cities (Fig. 5d) illustrate the patterns found in diverse climates: in Mediterranean Seattle WA and San Francisco CA, heating needs are sufficiently low that solar resources are comparable to or exceed heating needs in most months. (Note that about 55% of the resource is expected to be capturable with current technology, see Sec. S2.2 and Fig. S2-2.) In cold continental Chicago IL, Detroit MI, Albany NY, and Boston MA, useful solar resources are greatest in March and April at approximately 1.5 MWh/month per household, with lower resources of about 1 MWh/month found throughout the colder months of the heating season, and with solar resources exceeding heating needs in April, May, and October. In humid subtropical Washington DC and Philadelphia, similar resources of about 1.5 MWh/month per household peak earlier, in February and March; resources of about 1 MWh/month or more are available throughout the colder months. Finally, in cold semi-arid Reno and Denver, useful resources of about 1.5 MWh/month per household occur in five months of the year, diminishing only when heating needs decline.

Nationally, we estimate 2020 resources to be 770 ± 40 TWh. With current capture and retention efficiencies of 55% or more (Fig. S2-2), the scale of this untapped energy is comparable to one-third of the annual 1200 TWh U.S. residential heating need [81]. The 2020 value represents only a marginal decline from the 2000 estimate of 800 ± 50 TWh (Fig. S4-4), reflecting the fact that the NSHR is limited by solar resources rather than heating needs in some months and showing the influence of increasing household numbers [79].

Investigating the sensitivity of these results to collector area, we found that an increase to 20 m² substantially expanded the geographic area over which intercepted solar radiation equaled or exceeded the corresponding average heating need (shown for 2020 and 2000 in Fig. 6 and Fig. S4-5, respectively). For reference, the median residential photovoltaic array installed in 2018 occupied 35 m² of roof area [40]. Median household NSHR₂₀ values rose accordingly to 9.7 ± 2.4 MWh in 2020 (11.2 \pm 2.0 MWh in 2000), and corresponding national resources reached 1.09 ± 0.05 PWh in 2020 (1.16 ± 0.04 PWh in 2000); this doubling of collector area increased the proportion of resource to need from approx. 60% for the $\ensuremath{\text{NSHR}}_{10}$ to approx. 85% for the $\ensuremath{\text{NSHR}}_{20}$ in 2020 (\sim 55% to \sim 80% in 2000). In other words, the solar heating resource incident upon 20 m²-per-residence collector areas is of a scale comparable to four-fifths of the total residential space-heating energy use in the U.S. each year; the collectable, retainable energy equivalent, assuming the performance of current technology (Sec. S2.2 and Fig. S2-2), corresponds to nearly half of that need.

Further increases in collector area yielded progressively smaller increases in the ability to intercept useful resources as the NSHR approached the total space-heating energy need in each climate, revealing a pattern of diminishing returns with increasing collector area. This finding suggests that the exploration of optimal collector areas for site-specific combinations of climate, microclimate, building type, and cost will be valuable in the design of individual systems.

The net solar heating resource values described above are exceptional in the context of the space heating decarbonization dilemma. In the U.S., as well as in the industrialized world, space heating is such a sizable energy end-use that it cannot be ignored in economy-wide decarbonization plans [e.g. 115]. Efforts are therefore underway to promote the widespread electrification of space heating, relying on high-performance heat pumps powered by renewably generated electricity [e.g. 116]. While this approach is already very effective in mild climates with abundant wind, solar, and hydropower, it faces several challenges in colder climates and in regions with fossil fuel-dominated electricity generation [117,118]. One prominent issue is that even the most advanced heat pumps experience efficiency declines as outdoor air temperatures drop [57,119], requiring buildings in cold climates to maintain auxiliary systems and causing heat pump adoption

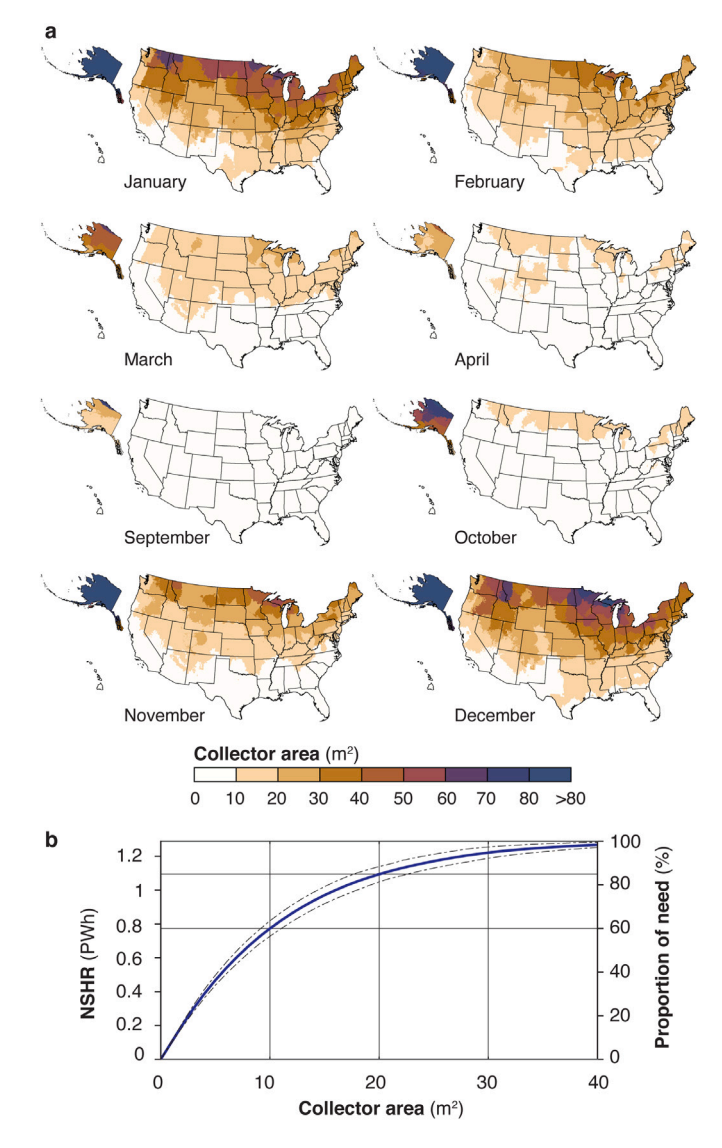


Fig. 6. Net solar heating resource sensitivity to collector area, 2020. (a) Areas ($\rm m^2$ per household) of optimally tilted surface required to intercept solar radiation equivalent to mean household heating needs in each of the eight coolest months: January–April and September–December. (b) NSHR $_{\alpha}$ (PWh and percent of national heating need) as a function of household collector area α , showing median values obtained with individual years of 1991–2005 NSRDB data [85] (solid line) and median absolute deviations (dashed lines); fine gridlines highlight values obtained with $10~\rm m^2$ and $20~\rm m^2$ collector areas, respectively. Tilts were optimized for $10~\rm m^2$ collector areas (shown in Fig. 4). Analogous data for 2000 are shown in Fig S4-5.

to face resistance in these areas [81]. Additionally, space heating electrification is expected to require cool and cold regions to expand their electricity delivery capacities substantially to meet new winter peak loads, although strategic fossil-fuel backup systems could alleviate part of this need [117]. Third, while U.S. solar and wind resources have the technical potential to generate electricity in quantities many times greater than current and projected demands [51], and while wind power generation aligns well with building space-heating needs [120], renewable power appears likely to comprise only 42%–54% of the total U.S. electricity production by 2050 [121]. As a result, space heating electrification alone is not likely to result in its decarbonization within the next several decades. Renewable energy technologies that can relieve pressure on electricity supplies are therefore extraordinarily valuable because they allow renewable power to be used for needs that can only be met with electricity.

3.5. Uncertainty and error

Uncertainty in the net solar heating resource estimates above was introduced principally by uncertainty in space heating energy use data [58,59]; in heating degree-days represented by weather files [73, 80]; and in interannual solar radiation variability [84,86]. These uncertainties potentially affected NSHR values indirectly through effects on tilt optima and directly through effects on heating needs and solar resources. Investigation revealed that effects related to tilt were negligible: among twenty cities representing five distinct climate types, optimal tilts derived for individual solar years [84] varied by <11° from optimal tilts reported in Fig. 4, and they improved NSHR₁₀ values by <50 kWh (i.e., <1%) in any given year (Fig. S5-1a). Variability in heating energy needs, reflecting interannual variation in monthly $HDD_{18.3^{\circ}C}$ \mathcal{H}_i and uncertainty in space-heating intensity ψ , affected tilt optima to a similarly small extent (Fig. S5-1b), with a similarly negligible effect on the NSHR₁₀. Both of these results are consistent with the observation that tilts within a 20° range centered on the optimum intercepted 97% of the net solar heating resource, while those within a 40° range intercepted 95%, showing that the reported optimal tilts represent the maxima of broad peaks (Fig. S5-2a).

The direct effect of heating season variability (i.e. \mathcal{H}_i) on heating need was more pronounced, affecting NSHR $_{10}$ values during milder months in which the useful resource was need-limited. Among the same twenty cities, interannual variability in 2020 heating season intensity (calculated as described in Section 2) yielded median absolute deviations of up to 11% (median=3%) in local NSHR $_{10}$ values, with the greatest sensitivity found in the mildest, most need-limited cities (Fig. S5-2b). At the national scale, this variability in \mathcal{H}_i affected aggregate NSHR $_{10}$ values by less than \pm 2%. Since space-heating energy intensities are expected to increase somewhat as winters warm and annual HDD decline, however [122,123], and since household numbers are rising [79], a clearer indication of national sensitivity to longer-term changes in \mathcal{H}_i is given by the comparison of NSHR $_{10}$ results for 2020 and 2000 (Fig. 5 and Fig. S4-4, respectively), quantified below.

Interannual solar radiation variability contributed the greatest uncertainty to NSHR₁₀ estimates, as $I_i(\theta, \alpha)$ values calculated for individual solar years [86] for the twenty cities showed median absolute deviations of over 20% in some months. Since this affected the NSHR only during months in which the resource was less than the heating need, however, annual NSHR_{10} values varied from the twelve-year medians by less than 8% (Fig. S5-3). Across much of the U.S., local annual NSHR₁₀ values were accordingly found to have median absolute deviations of $\leq 5\%$ of the total (Fig. 7 for 2020; Fig. S4-6 for 2000); higher values, approaching 14% of the total were found in the Upper Midwest and near the Pacific coast, reflecting variability in heating-season cloud cover. These corresponded to household median absolute deviations of ± 0.4 MWh for both 2020 and 2000, yielding NSHR₁₀ estimates of 7.0 ± 0.4 MWh for 2020 and 7.4 ± 0.4 MWh for 2000. Median absolute deviations of national resources, in turn, were found to be 40 TWh for 2020 and 50 TWh for 2000, yielding national NSHR₁₀ estimates of 770 ± 40 TWh in 2020 and 800 ± 50 TWh in 2000. These assessments also support a conservative estimate that household NSHR₁₀ values represent regional medians within $\pm 25\%$, with $\pm 11\%$ and $\pm 14\%$ accounting for the maximum documented effects of variability in heating need and in solar radiation availability, respectively.

4. Conclusions

The results above present compelling new evidence for an extensive, reliable, carbon-free renewable resource that is directly applicable to space-heating needs in a wide range of climate types. Virtually unexploited in the U.S., this net solar heating resource is needed urgently as rising built area, household numbers, and electricity demands sustain high space-heating emissions (Figs. S1-1 and S1-2), even as building envelopes improve, winters become milder, and renewable electricity

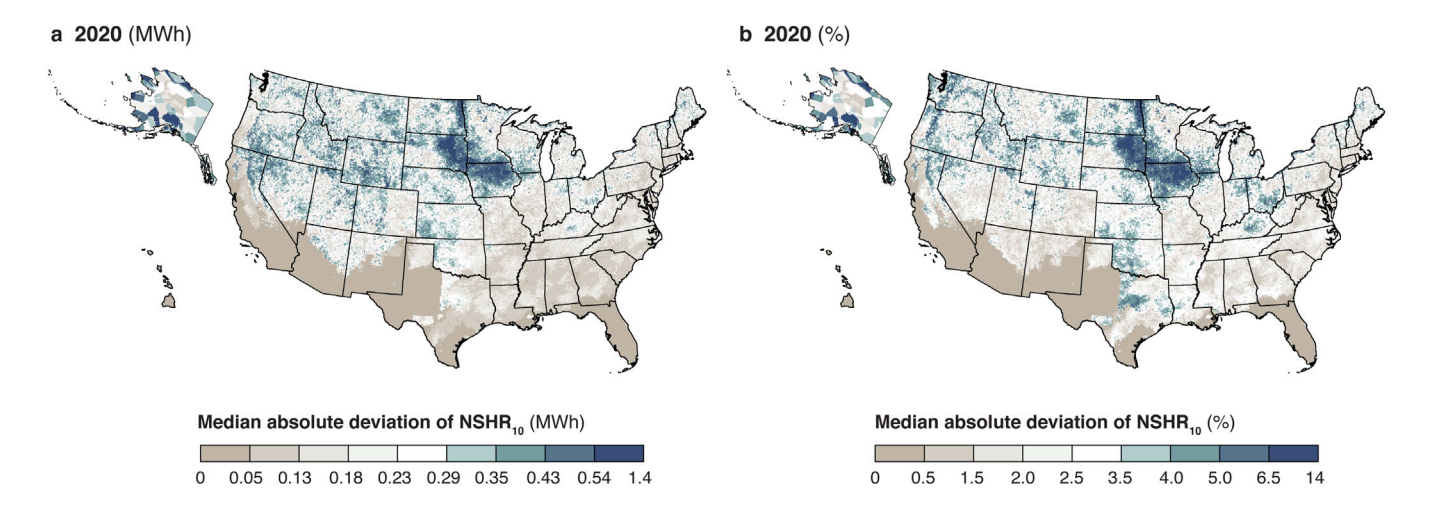


Fig. 7. NSHR sensitivity to solar radiation variability, 2020. Median absolute deviations of 2020 NSHR₁₀ values reflecting variation among individual years of 1998–2009 SolarAnywhere data [86] for the lower 48 contiguous states and Hawaii, and from National Solar Radiation Database solar data [87] for Alaska for the same years (1998–2009), in (a) MWh and (b) percentages of the NSHR₁₀. Analogous data for 2000 are shown in Fig. S4-6.

supplies increase. Because of its cool-season timing and its ability to use cloud-diffused solar radiation effectively, direct solar heating is also well-positioned to augment photovoltaic systems and heat pumps during winter months when heating, cooking, and lighting demands are greatest and when photovoltaic electricity production is lowest (Fig. S2-3).

We find direct solar heating resources to be substantial even in climates with cold or cloudy winters, including the humid continental Northeast and Midwest, cloudy continental Great Lakes region, humid subtropical Mid-Atlantic, Mediterranean Pacific Northwest and West Coast, and subarctic Alaska, within the U.S. In these climates, solar heat-collecting glass must be tilted significantly, within broad ranges, in response to the sky zenith-centered emission characteristic of diffuse solar radiation and to the higher solar altitudes found in longer heating seasons. Strikingly, diffuse solar radiation provides one-quarter or more of the total resource in these climates (Fig. 4). High solar intensities cause aggregate resources to be considerable, as well, in cities with warm humid subtropical and semi-arid climates (Fig. 5).

Space heating is by far the greatest energy end-use among U.S. residences, accounting for 1200 TWh of energy consumption and 300 million metric tons of CO_2 emissions each year (Fig. S1-2). Energy consumption per household, in turn, averages 10.3 MWh annually, varying from 0–25 MWh across the continental U.S. (see also Dataset S2). Among these climates, half of all household locations intercept annual useful solar heating resources of 7 MWh or more, with interannual variability of less than 15%, and numerous metropolitan areas have access to resources exceeding 5 TWh per year. Together, these yield a national resource of approximately 770 TWh annually (Fig. 6). Accounting for current solar heating system efficiencies of 55% or more (Figs. S2-1, S2-2), the capturable direct solar resource equals approximately one-third of current U.S. residential space-heating needs. The climate specificity of this investigation suggests further that comparable resources are likely to exist in comparable climates worldwide.

The values presented here describe resources to be sought. The ability of current direct solar systems to provide space-heating energy at 11 to 18 cents per kWh (Table S2-1), combined with the preponderance of low-rise housing stock in the U.S. [113], show that a substantial portion of this resource is available for immediate and cost-effective use. Additionally, improvements in glass properties that affect transmission and retention [124], and in the development of controls for effective storage and delivery of this energy [125], are ongoing. Together with the promise of further advances, the magnitude and extent of the net solar heating resource across diverse climate types supports a central role for direct solar heating in the development of carbon-free space heating strategies.

Code and product availability

MATLAB scripts for finding optimal tilt angles and calculating net solar heating resources are available in Zenodo (DOI: 10.5281/zenodo.3609326), as are the corresponding ArcMap 10.5 map packages (DOI: 10.5281/zenodo.3609306). High resolution interactive maps are also available on the University of Oregon ArcGIS website. In addition, 2020 station locations, space-heating energy use intensities, annual $\rm HDD_{18.3~^\circ C}$, optimal tilt angles, median and municipal NSHR $_{20}$ values, and their median absolute deviations are tabulated in Dataset S2. All other materials and products, including additional MATLAB scripts, WINDOW 7 glazing assembly specifications, and EnergyPlus models, are available upon request.

CRediT authorship contribution statement

A.R. Rempel: Conceptualization, Formal analysis, Funding acquisition, Methodology, Supervision, Visualization, Writing – original draft, Writing – review & editing. A.W. Rempel: Conceptualization, Formal analysis, Methodology, Software, Writing – original draft, Writing – review & editing. S.M. McComas: Formal analysis, Software, Visualization, Writing – original draft. S. Duffey: Formal analysis, Software, Visualization, Writing – original draft. C. Enright: Formal analysis, Methodology. S. Mishra: Conceptualization, Funding acquisition, Writing – review & editing.

Declaration of competing interest

The authors declare that they have no known competing financial interests or personal relationships that could have appeared to influence the work reported in this paper.

Acknowledgments

We gratefully acknowledge the contributions of Robert Bain, Alan Lai, and Josef Gordon to the development of spatial and analytical methods; of Ken Gates and John Reynolds to the development of underlying concepts; and of Judith Eisen, James Watkins, and Colin Meyer to the review and editing of the manuscript. This work was supported by the U.S. National Science Foundation (CBET-1804218).

Appendix A. Supplementary data

Supplementary material related to this article can be found online at https://doi.org/10.1016/j.rser.2021.111599.

References

- International Energy Agency. Energy efficiency indicators database. Technical report, Paris FR: International Energy Agency; 2020, http://www.iea.org/ reports/energy-efficiency-indicators-2020 [Accessed 30 January 2021].
- [2] International Energy Agency. Renewables 2019: Market analysis and forecast from 2019 to 2024: Heat. Technical report, Paris FR: International Energy Agency; 2019, http://www.iea.org/reports/renewables-2019/heat [Accessed 30 January 2021].
- [3] Creutzig F, Agoston P, Goldschmidt JC, Luderer G, Nemet G, Pietzcker RC. The underestimated potential of solar energy to mitigate climate change. Nature Energy 2017;2:17140.
- [4] Creutzig F, Roy J, Lamb WF, Azevedo IM, De Bruin WB, Dalkmann H, Edelenbosch OY, Geels FW, Grubler A, Hepburn C, et al. Towards demand-side solutions for mitigating climate change. Nature Clim Change 2018;8:260.
- [5] Reyna JL, Chester MV. Energy efficiency to reduce residential electricity and natural gas use under climate change. Nature Commun 2017;8:1–12.
- [6] Ellsworth-Krebs K. Implications of declining household sizes and expectations of home comfort for domestic energy demand. Nature Energy 2020;5:20-5.
- [7] Gao J, Zhong X, Cai W, Ren H, Huo T, Wang X, Mi Z. Dilution effect of the building area on energy intensity in urban residential buildings. Nature Commun 2019;10:1–9.
- [8] Jakob M, Steckel JC, Klasen S, Lay J, Grunewald N, Martínez-Zarzoso I, Renner S, Edenhofer O. Feasible mitigation actions in developing countries. Nature Clim Change 2014;4:961–8.
- [9] United Nations Environment Programme and International Energy Agency. 2019 Global Status Report for Buildings and Construction: Towards a zero-emissions, efficient, and resilient buildings and construction sector. Technical report, Global Alliance for Buildings and Construction; 2019, http://www.unenvironment.org/resources/publication/2019-global-statusreport-buildings-and-construction-sector [Accessed 30 January 2021].
- [10] van Ruijven BJ, De Cian E, Wing IS. Amplification of future energy demand growth due to climate change. Nature Commun 2019;10:1–12.
- [11] US Energy Information Administration. Annual energy outlook 2019. Technical report AEO2019, Washington, D.C.: U.S. Department of Energy; 2019, Table A4. Residential sector key indicators and consumption; http://www.eia.gov/ outlooks/archive/aeo19/ [Accessed 30 January 2021].
- [12] US Energy Information Administration. Annual energy outlook 2019. Technical report AEO2019, Washington, D.C.: U.S. Department of Energy; 2019, Table A19. Energy-related carbon dioxide emissions by end use; http://www.eia.gov/outlooks/archive/aeo19/ [Accessed 30 January 2021].
- [13] Lucon O, Ürge-Vorsatz D, Ahmed AZ, Akbari H, Bertoldi P, Cabeza LF, Eyre N, Gadgil A, Harvey LDD, Jiang Y, Liphoto E, Mirasgedis S, Murakami S, Parikh J, Pyke C, Vilariño MV. Ch. 9: Buildings. In: Edenhofer O, Pichs-Madruga R, Sokona Y, Farahani E, Kadner S, Seyboth K, Adler A, Baum I, Brunner S, Eickemeier P, Kriemann B, Savolainen J, Schlömer S, von Stechow C, Zwickel T, Minx J, editors. Climate change 2014: Mitigation of climate change. Contribution of working group III to the 5th assessment report of the Intergovernmental Panel on Climate Change. Cambridge, UK and New York, NY, USA: Cambridge University Press; 2014, p. 671–738.
- [14] Rempel AR. Chapter 11: Passive heating. In: Grondzik WA, Kwok AG, editors. Mechanical and electrical equipment for buildings. 13th ed.. John Wiley & Sons; 2019, p. 383–439.
- [15] American Society of Heating, Refrigerating, and Air-Conditioning Engineers. ANSI/ASHRAE/IES standard 90.1: Energy standard for buildings except low-rise residential buildings. Technical report, Atlanta, GA: American Society of Heating, Refrigerating, and Air-Conditioning Engineers; 2019.
- [16] Balcomb J, Barley D, McFarland R, Perry J, Wray W, Noll S. Passive solar design handbook, Volume 2: Passive solar design analysis. U.S. Department of Energy, Washington, D.C.: Los Alamos National Laboratory; 1980.
- [17] Swisher JN. Measured performance of passive solar buildings. Annu Rev Energy 1985;10:201–16.
- [18] Porteous C. Solar architecture in cool climates. Abingdon UK: Routledge Press; 2012.
- [19] MacGregor K. Potential for solar energy in northern climates. Int J Ambient Energy 1985;6:115–6.
- [20] MacGregor K. Is north really best for solar heating of buildings? In: Advances in solar energy technology. Elsevier; 1988, p. 3395–8.
- [21] Perez R, Ineichen P, Seals R, Michalsky J, Stewart R. Modeling daylight availability and irradiance components from direct and global irradiance. Sol Energy 1990;44:271–89.
- [22] Eymet V, Dufresne J, Ricchiazzi P, Fournier R, Blanco S. Long-wave radiative analysis of cloudy scattering atmospheres using a net exchange formulation. Atmos Res 2004;72:239–61.
- [23] Demain C, Journée M, Bertrand C. Evaluation of different models to estimate the global solar radiation on inclined surfaces. Renew Energy 2013;50:710–21.
- [24] Seifert RD. A solar design manual for Alaska. Technical report AK-RD-82-01, Fairbanks, AK: Institute of Water Resources, University of Alaska; 1981, http:// www.dot.state.ak.us/stwddes/research/assets/pdf/ak_rd_82_01.pdf [Accessed 30 January 2021].

- [25] Rempel A, Rempel A. Rocks, clays, water, and salts: Highly durable, infinitely rechargeable, eminently controllable thermal batteries for buildings. Geosciences 2013;3:63–101.
- [26] Bastien D, Athienitis AK. Passive thermal energy storage, part 1: Design concepts and metrics. Renew Energy 2018;115:1319–27.
- [27] Lawrence Berkeley National Laboratory. Windows & daylighting: Software tools: WINDOW documentation. 2019, windows.lbl.gov/tools/window/documentation [Accessed 30 January 2021].
- [28] National Renewable Energy Laboratory. EnergyPlus V8.7, energyplus.net. 2016, Building Technologies Office, U.S. Department of Energy, Washington D.C..
- [29] Crawley DB, Lawrie LK, Winkelmann FC, Buhl WF, Huang YJ, Pedersen CO, Strand RK, Liesen RJ, Fisher DE, Witte MJ, et al. EnergyPlus: Creating a new-generation building energy simulation program. Energy Build 2001;33:319–31.
- [30] USDepartment of Energy. EnergyPlus version 8.9.0 documentation: Engineering reference. Technical report, Washington, D.C.: Building Technologies Office, U.S. Department of Energy; 2018, bigladdersoftware.com/epx/docs/8-9/engineering-reference/ [Accessed 30 January 2021].
- [31] Rempel AR, Rempel AW, Cashman KV, Gates KR, Page CJ, Shaw B. Interpretation of passive solar field data with EnergyPlus models: Un-conventional wisdom from four sunspaces in Eugene, Oregon. Build Environ 2013;60:158–72.
- [32] Rempel AR, Bertis S, Farnham S, Pearson Z, Seipp C, Valcour D, Holmes O. Restorative passive solar redesign in Upstate New York. In: Proceedings of the 32nd International Conference on Passive and Low-energy Architecture. Los Angeles CA; 2016. p. 1872–8.
- [33] Zirnhelt HE, Richman RC. The potential energy savings from residential passive solar design in Canada. Energy Build 2015;103:224–37.
- [34] Stevanović S. Optimization of passive solar design strategies: A review. Renew Sustain Energy Rev 2013;25:177–96.
- [35] Liu Z, Wu D, Yu H, Ma W, Jin G. Field measurement and numerical simulation of combined solar heating operation modes for domestic buildings based on the Qinghai–Tibetan plateau case. Energy Build 2018;167:312–21.
- [36] Wetter M. Generic optimization program user manual version 3.0.0. Technical report, Berkeley, CA (United States): Lawrence Berkeley National Lab.(LBNL); 2009.
- [37] Wetter M. Co-simulation of building energy and control systems with the building controls virtual test bed. J Build Perform Simul 2011;4:185–203.
- [38] Dostal J. Energyplus co-simulation toolbox: Co-simulation of EnergyPlus models in MATLAB/simulink. 2020, https://github.com/dostaji4/EnergyPlus-co-simulation-toolbox [Accessed 30 January 2021].
- [39] Rempel AR, Lim S. Numerical optimization of integrated passive heating and cooling systems yields simple protocols for building energy decarbonization. Sci Technol Built Environ 2019;25:1226–36.
- [40] Barbose G, Darghouth N, Elmallah S, Forrester S, Kristina SH K, Millstein D, Rand J, Cotton W, Sherwood S, O'Shaughnessy E. Tracking the sun: Pricing and design trends for distributed photovoltaic systems in the United States: 2019 edition. 2019, https://emp.lbl.gov/tracking-the-sun [Accessed 30 January 2021].
- [41] Doheny M, editor. Assemblies costs with RSMeans data. 44th ed.. Gordian Construction Publishers; 2019.
- [42] US Census Bureau. AMerican community survey: House heating fuels. 2018, TableID: B25040 https://data.census.gov/cedsci/ [Accessed 30 January 2021].
- [43] International Code Council. International energy conservation code. 2018, https://codes.iccsafe.org/content/IECC2018P4 [Accessed 30 January 2021].
- [44] International Code Council. International Green Construction Code. Washington, D.C.: International Code Council; 2018.
- [45] US Green Building Council. Leadership in energy and environmental design (LEED) v4. 2016, https://www.usgbc.org/leed/v4 [Accessed 30 January 2021].
- [46] US Department of Energy. Building america program. 2020, Office of Energy Efficiency and Renewable Energy, https://www.energy.gov/eere/buildings/ building-america [Accessed 30 January 2021].
- [47] US Environmental Protection Agency and the US Department of Energy. Energy star certification for buildings. 2020, https://www.energystar.gov/buildings/ facility-owners-and-managers/existing-buildings/earn-recognition/energy-starcertification [Accessed 30 January 2021].
- [48] Passive House Institute US. PHIUS+ certification overview. 2021, https://www.phius.org/phius-certification-for-buildings-products/project-certification/overview [Accessed 30 January 2021].
- [49] Garrett V, Koontz TM. Breaking the cycle: Producer and consumer perspectives on the non-adoption of passive solar housing in the U.S.. Energy Policy 2008;36:1551–66.
- [50] DeKay M, Brown GZ. Chapter B7: Passive solar buildings, and appendix E49: Sunspaces. In: Sun, wind, and light: Architectural design strategies. John Wiley & Sons; 2014, 208–9 and E.134–5.
- [51] Lopez A, Roberts B, Heimiller D, Blair N, Porro G. US renewable energy technical potentials. A GIS-based analysis. Technical report, National Renewable Energy Lab.(NREL), Golden, CO (United States); 2012.
- [52] Gagnon P, Margolis R, Melius J, Phillips C, Elmore R. Estimating rooftop solar technical potential across the U.S. using a combination of GIS-based methods, lidar data, and statistical modeling. Environ Res Lett 2018;13:024027.

- [53] Singh T, Hussien MAA, Al-Ansari T, Saoud K, McKay G. Critical review of solar thermal resources in GCC and application of nanofluids for development of efficient and cost effective CSP technologies. Renew Sustain Energy Rev 2018;91:708–19.
- [54] US Energy Information Administration. Hourly electricity consumption varies throughout the day and across seasons. 2020, http://www.eia.gov/ todayinenergy/detail.php?id=42915 [Accessed 30 January 2021].
- [55] National Oceanic and Atmospheric Administration. Comparative climatic data for the United States through 2018. Technical report, Asheville NC: National Centers for Environmental Information; 2018, http://www.ncdc.noaa.gov/sites/ default/files/attachments/CCD-2018.pdf [Accessed 2 February 2021].
- [56] National Renewable Energy Laboratory. PVWatts calculator, v6.1.3. 2020, Office of Energy Efficiency and Renewable Energy, U.S. Department of Energy, Golden CO, pvwatts.nrel.gov/index.php [last accessed 30 January 2021].
- [57] Schoenbauer B, Kessler N, Bohac D, Kushler M. Field assessment of cold climate air source heat pumps. In: American Council for an Energy-Efficient Economy (ACEE) Summer Study on Energy Efficiency in Buildings. 2016, http: //www.aceee.org/files/proceedings/2016/data/papers/1_700.pdf [Accessed 30 January 2021].
- [58] US Energy Information Administration. Residential energy consumption survey: Table CE3.1: Annual household site end-use consumption in the U.S.-totals and averages, 2015, U.S. Department of Energy, Washington, D.C.. 2018, http:// www.eia.gov/consumption/residential/data/2015/c&e/pdf/ce3.1.pdf [Accessed 30 January 2021].
- [59] US Energy Information Administration. Residential energy consumption survey: Table CE2-1c. Space-heating energy consumption in U.S. households by climate zone, 2001, U.S. Department of Energy, Washington D.C.. 2001, http://www.eia.gov/consumption/residential/data/2001/pdf/ce/ spaceheat/ce2-1c_climate2001.pdf [Accessed 30 January 2021].
- [60] Ranson M, Morris L, Kats-Rubin A. Climate change and space heating energy demand: A review of the literature. Technical report 14–07, National Center for Environmental Economics, Washington D.C.: U.S. Environmental Protection Agency: 2014.
- [61] Confidential information protection and statistical efficiency act (CIPSEA). 2002, Congressional Record Vol. 148, 116 STAT. 2962, Public Law 107–347, Washington, D.C..
- [62] US Energy Information Administration. Annual report on implementation of CIPSEA, U.S. Department of Energy, Washington, D.C.. 2015, http://www.eia. gov/about/pdfs/2015_cipsea_report.pdf [Accessed 30 January 2021].
- [63] US Energy Information Administration. Residential energy consumption survey: 2001 RECS survey data: Methodology, U.S. Department of Energy, Washington D.C.. 2001, http://www.eia.gov/consumption/residential/data/2001/index. php?view=methodology [Accessed 30 January 2021].
- [64] US Energy Information Administration. Commercial buildings energy consumption survey: Maps, U.S. Department of Energy, Washington D.C.. 2019, http://www.eia.gov/consumption/commercial/maps.php#2003climate [Accessed 30 January 2021].
- [65] US Energy Information Administration. Residential energy consumption survey: RECS 2015 survey data: Methodology, U.S. Department of Energy, Washington, D.C.. 2015, http://www.eia.gov/consumption/residential/data/2015/index.php?view=methodology [Accessed 30 January 2021].
- [66] US Census Bureau. Geographies: Cartographic boundary files: 2010 counties. 2010, http://www.census.gov/geographies/mapping-files/time-series/geo/carto-boundary-file.2010.html, File: gz_2010_us_050_00_500k.zip, [Accessed 30 January 2021].
- [67] Esri Inc. ArcGIS v10.5. 2019, Redlands, CA, desktop.arcgis.com/en/ [Accessed 30 January 2021].
- [68] Altman DG, Bland JM. Standard deviations and standard errors. BMJ 2005;331:903
- [69] Wilcox S, Marion W. User's manual for TMY3 data sets. Technical report NREL/TP-581-43156, Golden, CO: National Renewable Energy Laboratory, U.S. Department of Energy; 2008, https://www.nrel.gov/docs/fy08osti/43156.pdf [Accessed 30 January 2021].
- [70] National Renewable Energy Laboratory. National solar radiation database archives, 1961-1990: Typical meteorological year 2. 1995, U.S. Department of Energy, Office of Energy Efficiency and Renewable Energy, Golden CO, https://nsrdb.nrel.gov/data-sets/archives.html [Accessed 30 January 2021].
- [71] Sustainable Energy Research Group. CCWorldWeatherGen: Climate change world weather file generator, version 1.8. 2013, University of Southampton, Energy and Climate Change Division, Southampton UK, https://energy.soton. ac.uk/ccworldweathergen/ [Accessed 30 January 2021].
- [72] Moazami A, Carlucci S, Geving S. Critical analysis of software tools aimed at generating future weather files with a view to their use in building performance simulation. Energy Procedia 2017;132:640–5.
- [73] Jentsch MF, James PA, Bourikas L, Bahaj AS. Transforming existing weather data for worldwide locations to enable energy and building performance simulation under future climates. Renew Energy 2013;55:514–24.
- [74] Crawley D, Lawrie L. Climate.OneBuilding.org: WMO region 4: North and Central America TMYx 2004–2018 weather files. 2019, http://www.climate.onebuilding.org/WMO_Region_4_North_and_Central_America/USA_United_States_of_America/index.html [Accessed 30 January 2021].

- [75] National Renewable Energy Laboratory. U.S. TMY3 boundaries. 2011, U.S. Department of Energy, Office of Energy Efficiency and Renewable Energy, Golden CO, https://openei.org/wiki/File:NREL-tmy3-boundary-01.pdf [Accessed 30 January 2021].
- [76] US Geological Survey. North America elevation 1-kilometer resolution GRID. 2007, http://www.sciencebase.gov/catalog/item/4fb5495ee4b04cb937751d6d, File: Elevation_GRID.zip [Accessed 30 January 2021].
- [77] National Climatic Data Center. 1981-2010 temperature normals: Standard deviations. 2011, http://www1.ncdc.noaa.gov/pub/data/normals/1981-2010/products/temperature/mly-tavg-stddev.txt [Accessed 2 February 2021].
- [78] National Oceanographic and Atmospheric Administration. Climate data online: Surface data hourly. 2019, https://www7.ncdc.noaa.gov/CDO/cdo [Accessed 2 February 2021].
- [79] Manson S, Schroeder J, Riper DV, Ruggles S. IPUMS National historical geographic information system (NHGIS) version 14.0: U.S. census data tables and mapping files [database]. 2019, ipums.org/projects/ipums-nhgis/d050.v14.0 [Accessed 30 January 2021].
- [80] National Renewable Energy Laboratory. Weather data by region:
 North and central america WMO region 4 USA: Typical meteorological year (TMY) 3. 2008, energyplus.net/weather-region/north_and_central_america_wmo_region_4/USA%20%20 [Accessed 30 January 2021].
- [81] US Energy Information Administration. Residential energy consumption survey, U.S. Department of Energy, Washington, D.C.. 2015, http://www.eia.gov/ consumption/residential/data/2015/ [Accessed 2 February 2021].
- [82] US Energy Information Administration. Residential energy consumption survey, U.S. Department of Energy, Washington D.C.. 2001, http://www.eia.gov/consumption/residential/data/2001/ [Accessed 30 January 2021].
- [83] Fieller EC. Some problems in interval estimation. J R Stat Soc Ser B Stat Methodol 1954;16:175–85.
- [84] National Renewable Energy Laboratory. National solar radiation database 1991—2005 update: User's manual. Technical report NREL/TP-581-41364, Golden CO: U.S. Department of Energy; 2007, http://www.nrel.gov/docs/fy07osti/41364.pdf [Accessed 30 January 2021].
- [85] National Renewable Energy Laboratory. National solar radiation database 1991—2005 update datafiles. 2007, OpenEI: Energy Information Datasets: https://openei.org/datasets/files/39/pub/ [Accessed 30 January 2021].
- [86] National Centers for Environmental Information. National solar radiation database SolarAnywhere 10 km model output for 1989 to 2009. 2018, https://catalog.data.gov/dataset/national-solar-radiation-database-nsrdb-solaranywhere-10-km-model-output-for-1989-to-2009 [Accessed 2 February, 2021]
- [87] National Renewable Energy Laboratory. National solar radiation data base: 1991–2010 update. 2012, National Centers for Environmental Information, National Oceanographic and Atmospheric Administration, Washington D.C., https://www.ncdc.noaa.gov/data-access/land-based-station-data/ land-based-datasets/solar-radiation, [Accessed 2 February 2021].
- [88] Wilcox S. National solar radiation database 1991-2010 update: User's manual. Technical report NREL/TP-5500-54824, Golden, CO: National Renewable Energy Laboratory, U.S. Department of Energy; 2012, https://www.nrel.gov/docs/fy12osti/54824.pdf [Accessed 30 January 2021].
- [89] Myers D, Wilcox S, Marion W, George R, Anderberg M. Broadband model performance for an updated national solar radiation database in the United States of America. Technical report NREL/CP-560-37699, Golden CO, United States: National Renewable Energy Laboratory; 2005.
- [90] Gueymard CA, Wilcox SM. Assessment of spatial and temporal variability in the U.S. solar resource from radiometric measurements and predictions from models using ground-based or satellite data. Sol Energy 2011;85:1068–84.
- [91] MATLAB. V.9.4 (R2018a). Natick, Massachusetts: The MathWorks, Inc.; 2018.
- [92] Conover W. Practical nonparametric statistics. 3rd ed.. New York: John Wiley & Sons; 1999.
- [93] Kannan N, Vakeesan D. Solar energy for future world: A review. Renew Sustain Energy Rev 2016;62:1092–105.
- [94] Kabir E, Kumar P, Kumar S, Adelodun AA, Kim K-H. Solar energy: Potential and future prospects. Renew Sustain Energy Rev 2018;82:894–900.
- [95] Perez R, Kivalov S, Schlemmer J, Hemker Jr K, Renné D, Hoff TE. Validation of short and medium term operational solar radiation forecasts in the U.S.. Sol Energy 2010;84:2161–72.
- [96] Rempel AR, Rempel AW, Gates KR, Shaw B. Climate-responsive thermal mass design for Pacific Northwest sunspaces. Renew Energy 2016;85:981–93.
- [97] Athienitis A, Santamouris M. Thermal Analysis and Design of Passive Solar Buildings. Taylor and Francis; 2013.
- [98] Navarro L, de Gracia A, Niall D, Castell A, Browne M, McCormack SJ, Griffiths P, Cabeza LF. Thermal energy storage in building integrated thermal systems: A review. Part 2. Integration in passive systems. Renew Energy 2016;85:1334–56.
- [99] Ferrando M, Causone F, Hong T, Chen Y. Urban building energy modeling (UBEM) tools: A state-of-the-art review of bottom-up physics-based approaches. Sustainable Cities Soc 2020;102408.

- [100] École Polytechnique Fédérale de Lausanne (EPFL). CitySim. 2009, https://www.epfl.ch/labs/leso/transfer/software/citysim/ [Accessed 30 January 2021].
- [101] MIT Sustainable Design Laboratory. Urban modeling interface (UMI). 2013, Cambridge, MA, http://web.mit.edu/sustainabledesignlab/projects/umi/ [Accessed 30 January 2021].
- [102] Lawrence Berkeley National Laboratory (LBNL). CityBES. 2015, Berkeley, CA, https://citybes.lbl.gov/#citybes [Accessed 30 January 2021].
- [103] Chen Y, Hong T, Piette MA. Automatic generation and simulation of urban building energy models based on city datasets for city-scale building retrofit analysis. Appl Energy 2017;205:323–35.
- [104] ETH-Zurich. City energy analyst (CEA). 2016, Zurich, CH, https: //cityenergyanalyst.com/ [Accessed 30 January 2021].
- [105] Gagnon P, Margolis R, Melius J, Phillips C, Elmore R. Rooftop solar photovoltaic technical potential in the United States: A detailed assessment. Technical report, National Renewable Energy Lab.(NREL), Golden, CO (United States); 2016, http://www.nrel.gov/docs/fy16osti/65298.pdf [Accessed 30 January 2021].
- [106] Lechner N. Chapter 7: Passive solar. In: Heating, Cooling, Lighting: Sustainable Design Methods for Architects. John Wiley & Sons; 2014, p. 165–96.
- [107] International Commission on Illumination (CIE). Spatial distribution of daylight: CIE standard general sky. 2004, ISO 15469:2004(E)/CIE S 011/E:2003, Geneva, Switzerland.
- [108] Carmody J, Arasteh D, Selkowitz S, Heschong L. Residential windows: A guide to new technologies and energy performance. WW Norton & Company; 2007.
- [109] Chinazzo G, Wienold J, Andersen M. Daylight affects human thermal perception. Sci Rep 2019;9:1–15.
- [110] te Kulve M, Schlangen L, van Marken Lichtenbelt W. Interactions between the perception of light and temperature. Indoor Air 2018;28:881–91.
- [111] Van Esch M, Looman R, de Bruin-Hordijk G. The effects of urban and building design parameters on solar access to the urban canyon and the potential for direct passive solar heating strategies. Energy Build 2012;47:189–200.
- [112] Sanaieian H, Tenpierik M, Van Den Linden K, Seraj FM, Shemrani SMM. Review of the impact of urban block form on thermal performance, solar access and ventilation. Renew Sustain Energy Rev 2014;38:551–60.
- [113] National Multifamily Housing Council. Resident demographics: Metropolitan areas: Population, housing, and renters. 2017, http://www.nmhc.org/research-insight/quick-facts-figures/quick-facts-resident-demographics/#Metropolitan_ Areas [Accessed 30 January 2021].

- [114] Voss K. Solar energy in building renovation-results and experience of international demonstration buildings. Energy Build 2000;32:291–302.
- [115] Jacobson MZ, Delucchi MA, Bauer ZA, Goodman SC, Chapman WE, Cameron MA, Bozonnat C, Chobadi L, Clonts HA, Enevoldsen P, et al. 100% clean and renewable wind, water, and sunlight all-sector energy roadmaps for 139 countries of the world. Joule 2017;1:108–21.
- [116] International Energy Agency. Tracking report: Tracking buildings: Heating. 2020, Paris, FR, http://www.iea.org/reports/heating [Accessed 2 February 2021].
- [117] Waite M, Modi V. Electricity load implications of space heating decarbonization pathways. Joule 2020;4:376–94.
- [118] Vaishnav P, Fatimah AM. The environmental consequences of electrifying space heating. Environ Sci Technol 2020:54:9814–23.
- [119] Shen B, Baxter VD, Abdelaziz O, Rice CK. Finalize field testing of cold climate heat pump (CCHP) based on tandem vapor injection compressors. 2017, http://dx.doi.org/10.2172/1357984, http://www.osti.gov/biblio/1357984.
- [120] Jacobson MZ. On the correlation between building heat demand and wind energy supply and how it helps to avoid blackouts. Smart Energy 2021;1:100009.
- [121] USEnergy Information Administration. Annual energy outlook 2021. Technical report AEO2021, Washington, D.C.: U.S. Department of Energy; 2021, http: //www.eia.gov/outlooks/aeo/pdf/AEO_Narrative_2021.pdf [Accessed 27 July 2021]
- [122] Sorrell S, Dimitropoulos J, Sommerville M. Empirical estimates of the direct rebound effect: A review. Energy Policy 2009;37:1356–71.
- [123] Greening LA, Greene DL, Difiglio C. Energy efficiency and consumption—the rebound effect—a survey. Energy Policy 2000;28:389–401.
- [124] Wang S, Xu Z, Wang T, Xiao T, Hu X-Y, Shen Y-Z, Wang L. Warm/cool-tone switchable thermochromic material for smart windows by orthogonally integrating properties of pillar[6]arene and ferrocene. Nature Commun 2018;9:1–9.
- [125] Wen JT, Mishra S. Intelligent building control systems. Springer; 2018.